Supplementary figures and figure legends

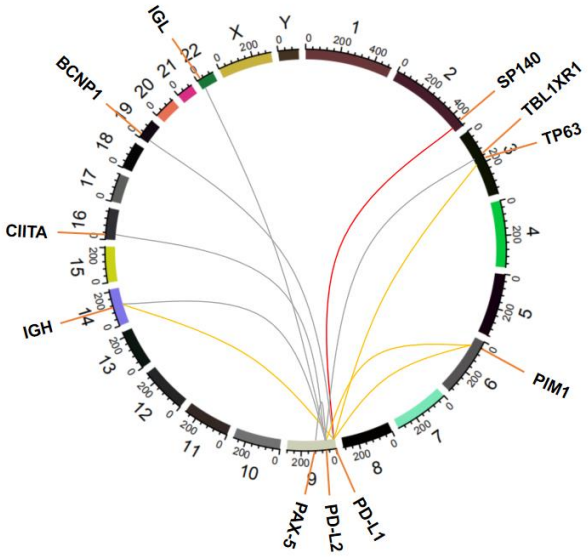

Figure S1. Summary of known translocations involving the PD-L1/L2 loci and one novel gene fusion in diffuse large B-cell lymphoma. Translocations involving PD-L1/L2 loci demonstrated by other investigators are depicted in gray, and those characterized by a previous study of ours are depicted in orange. The novel gene fusion identified in our study is depicted in red.

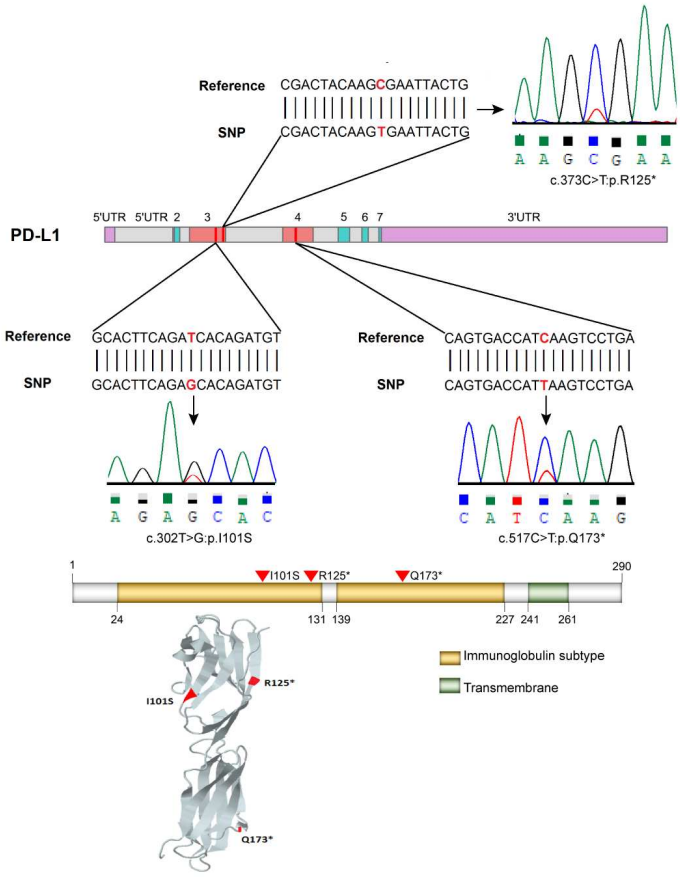

Figure S2. Schematic representation of PD-L1 showing the locations of alterations. Distribution of PD-L1 alterations identified by targeted deep sequencing and subsequently validated via Sanger sequencing in genomic and protein maps showing the locations and variations of nucleotide/amino acid substitutions. The protein 3D structure of PD-L1 was obtained from the Missense 3D database.

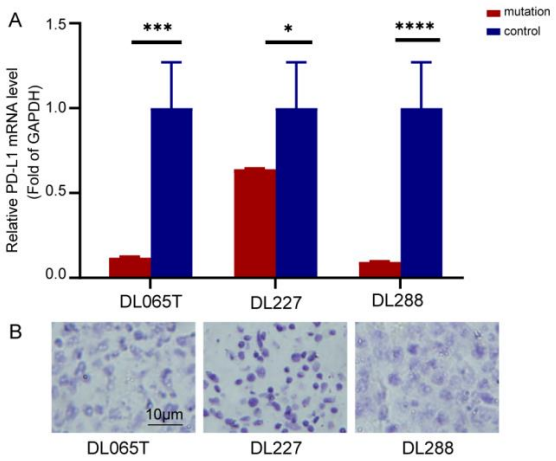

Figure S3. Expression of PD-L1 in samples with PD-L1 genetic mutations. (A) Relative PD-L1 mRNA expression in samples with PD-L1 genetic mutations. Three samples of patients with lymphoproliferative diseases were used as a control. (B) PD-L1 immunostaining in samples with PD-L1 genetic mutations. The images were captured at 400× magnification. * = $p < 0.05$, *** = $p < 0.0001$, **** = $p < 0.00001$.

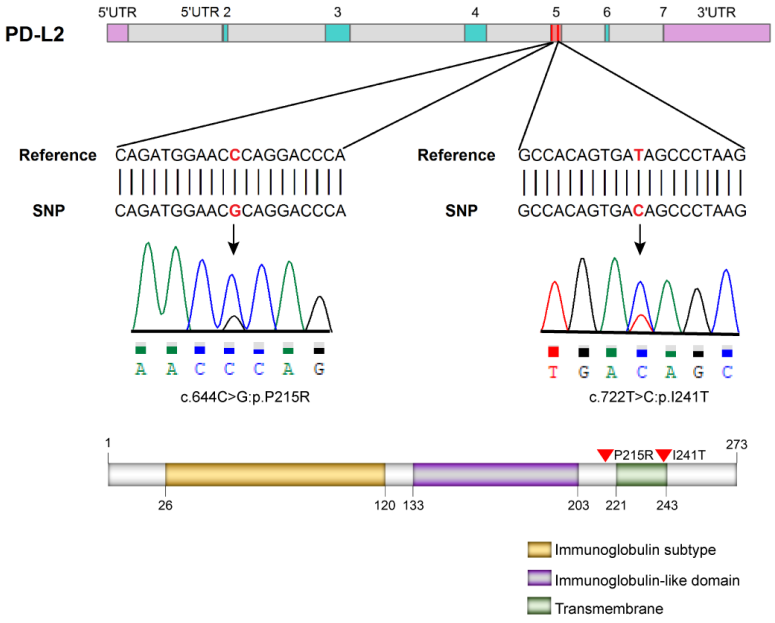

Figure S4. Schematic representation of PD-L2 showing the locations of alterations. Distribution of PD-L2 alterations identified by targeted deep sequencing and subsequently validated by Sanger sequencing in genomic and protein maps showing locations and variations of nucleotide/amino acid substitutions. The protein 3D structure of PD-L2 was not obtained from the Missense 3D database.

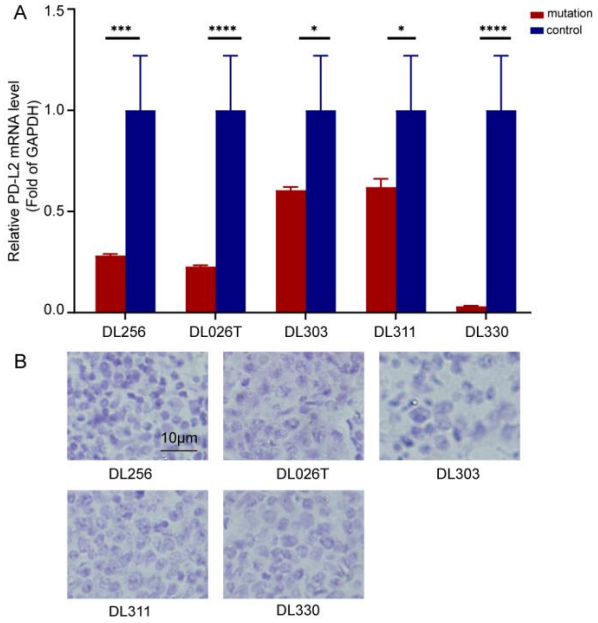

Figure S5. PD-L2 expression in samples with PD-L2 genetic mutations. (A) Relative PD-L2 mRNA expression in samples with PD-L2 genetic mutations. Three samples of patients with lymphoproliferative diseases were used as a control. (B) PD-L2 immunostaining in samples with PD-L2 genetic mutations. Images were captured at 400× magnification. * = $p < 0.05$, *** = $p < 0.0001$, **** = $p < 0.00001$.

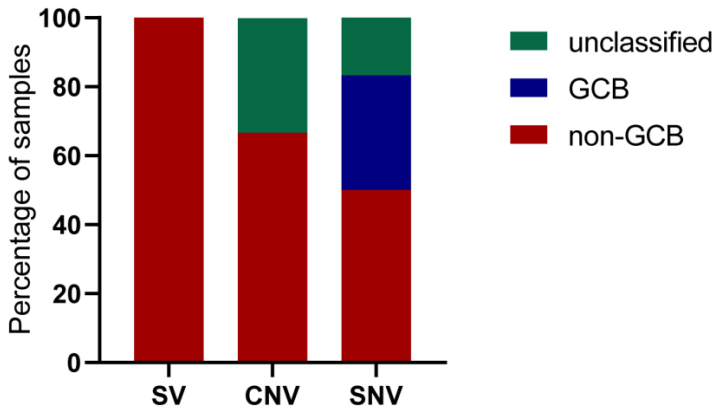

Figure S6. Distribution of diffuse large B-cell lymphoma subtypes in different genetic alterations, including SVs (n=2), CNVs (n = 3), and SNVs (n=12). SVs: structural variations; CNVs: copy number variations; SNVs: single nucleotide variants.

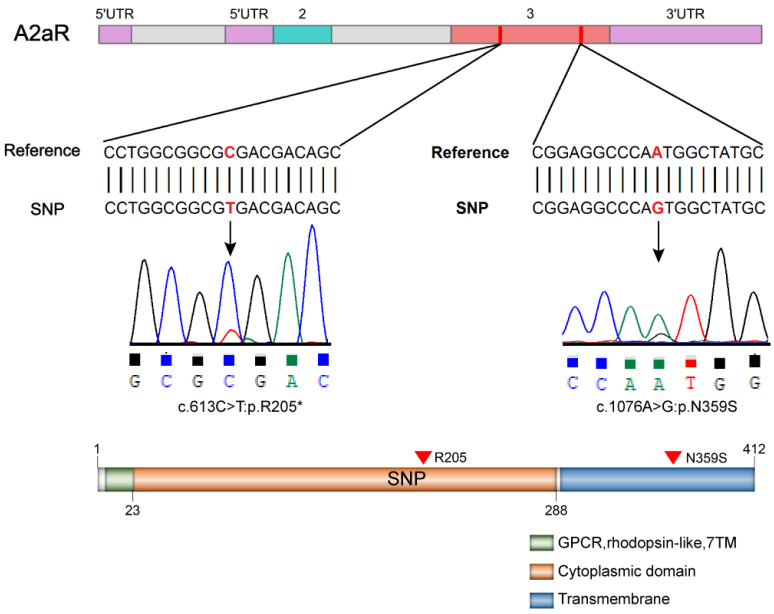

Figure S7. Schematic representation of A2aR showing the locations of alterations.

Distribution of A2aR alterations identified by targeted deep sequencing and subsequently validated by Sanger sequencing in genomic and protein maps showing the locations and variations of nucleotide/amino acid substitutions. The protein 3D structure of A2aR was not obtained from the Missense 3D database.

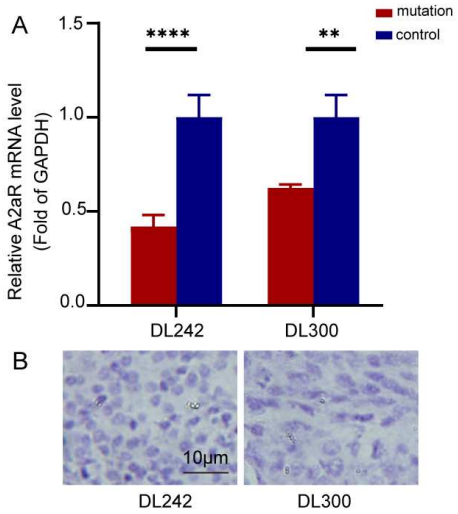

Figure S8. A2aR expression in samples with A2aR genetic mutations. (A) Relative A2aR mRNA expression in samples with A2aR genetic mutations. Three samples of patients with lymphoproliferative diseases were used as a control. (B) A2aR immunostaining in samples with A2aR genetic mutations. The images were captured at 400× magnification. ** = $p < 0.001$, **** = $p < 0.00001$.

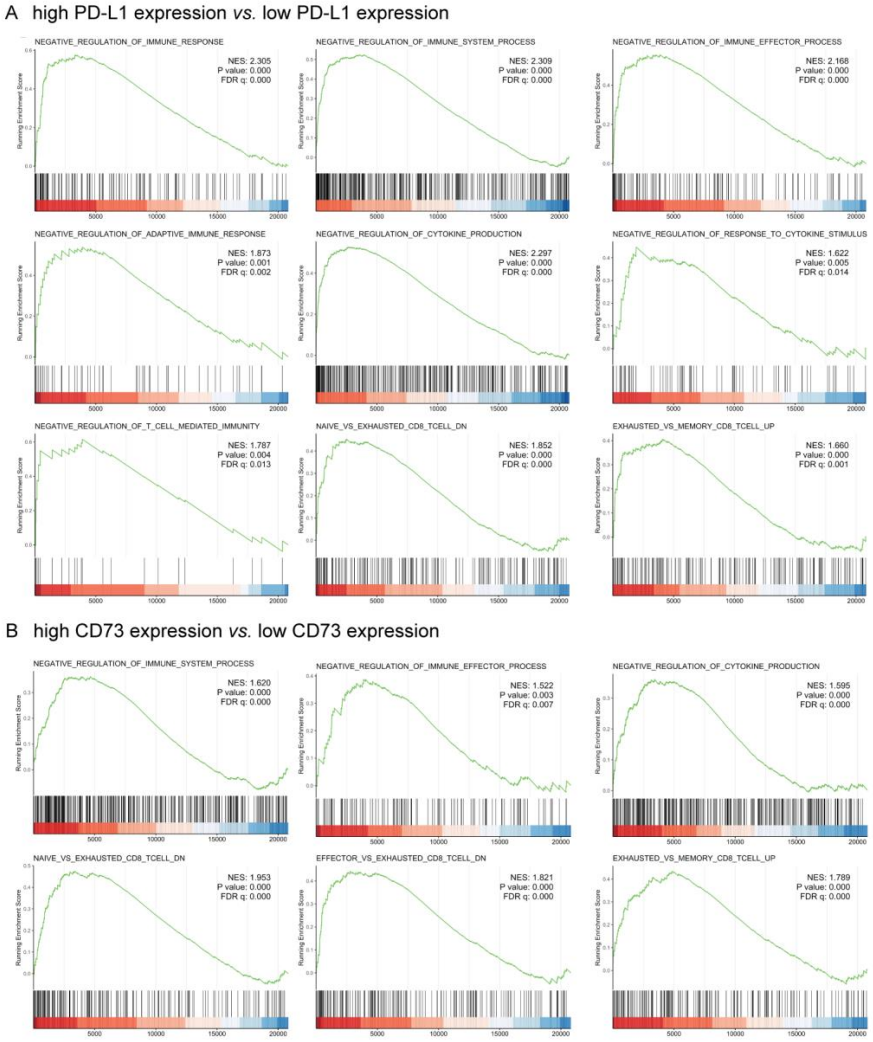

Figure S9. Significantly enriched gene sets involved in negatively regulating the immune response in the high PD-L1 (A) / CD73 (B) expression group versus the low PD-L1/CD73 expression group by gene set enrichment analysis in the GSE117556 cohort. $|NES|>1$, $p\ value < 0.05$, and $FDR\ q\ value < 0.05$ were considered statistically significant. NES: normalized enrichment score, FDR: false discovery rate.

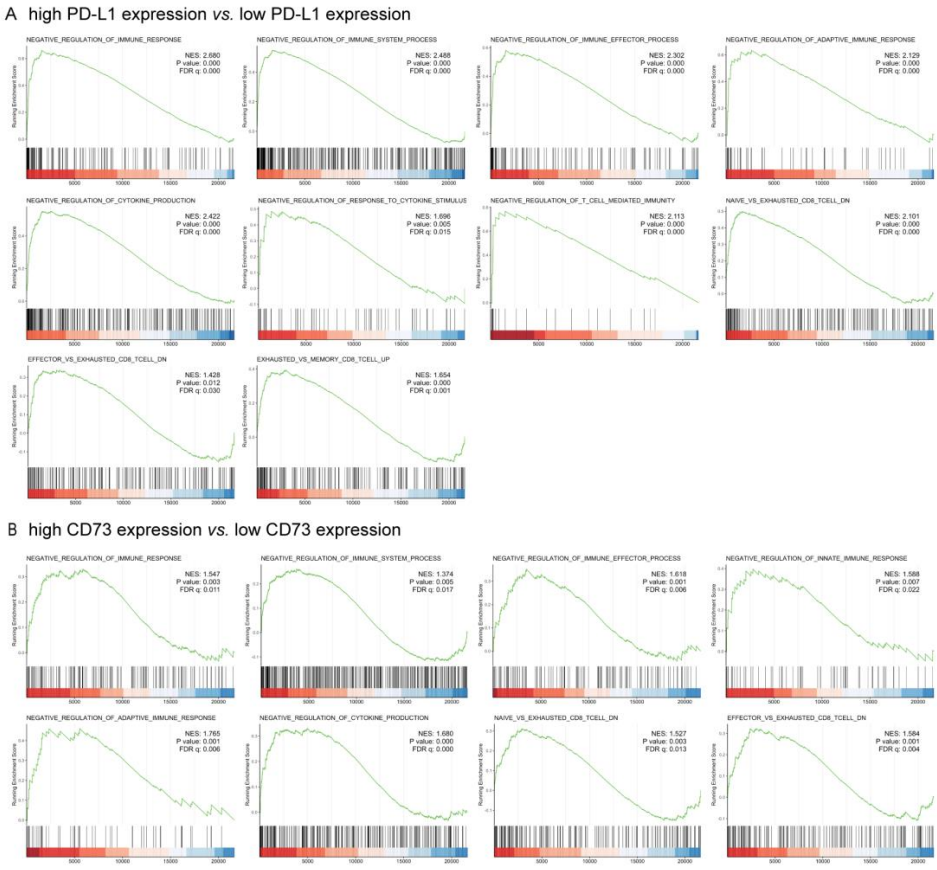

Figure S10. Significantly enriched gene sets involved in negatively regulating the immune response in the high PD-L1 (A) / CD73 (B) expression group versus the low PD-L1/CD73 expression group by gene set enrichment analysis in the GSE31312 cohort. $|NES|>1$, $p\ value < 0.05$, and $FDR\ q\ value < 0.05$ were considered statistically significant. NES: normalized enrichment score, FDR: false discovery rate.

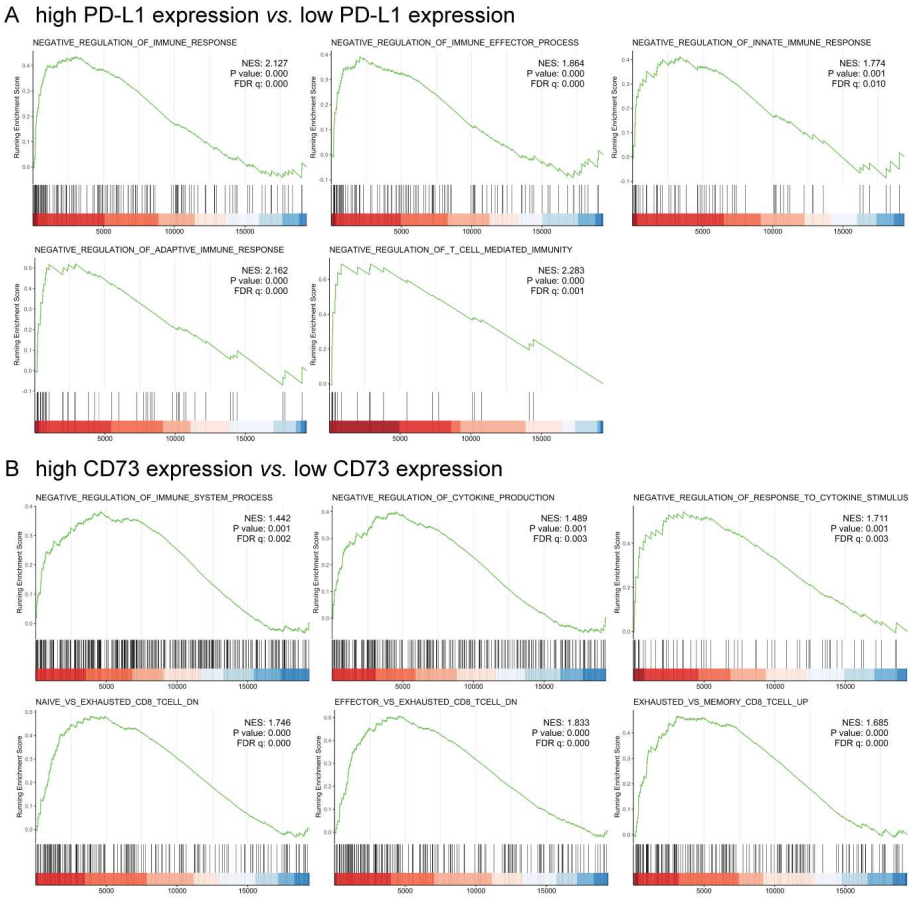

Figure S11. Significantly enriched gene sets involved in negatively regulating the immune response in the high PD-L1 (A) / CD73 (B) expression group versus the low PD-L1/CD73 expression group by gene set enrichment analysis in the GSE147986 cohort. $|NES|>1$, $p\ value < 0.05$, and $FDR\ q\ value < 0.05$ were considered statistically significant. NES: normalized enrichment score, FDR: false discovery rate.

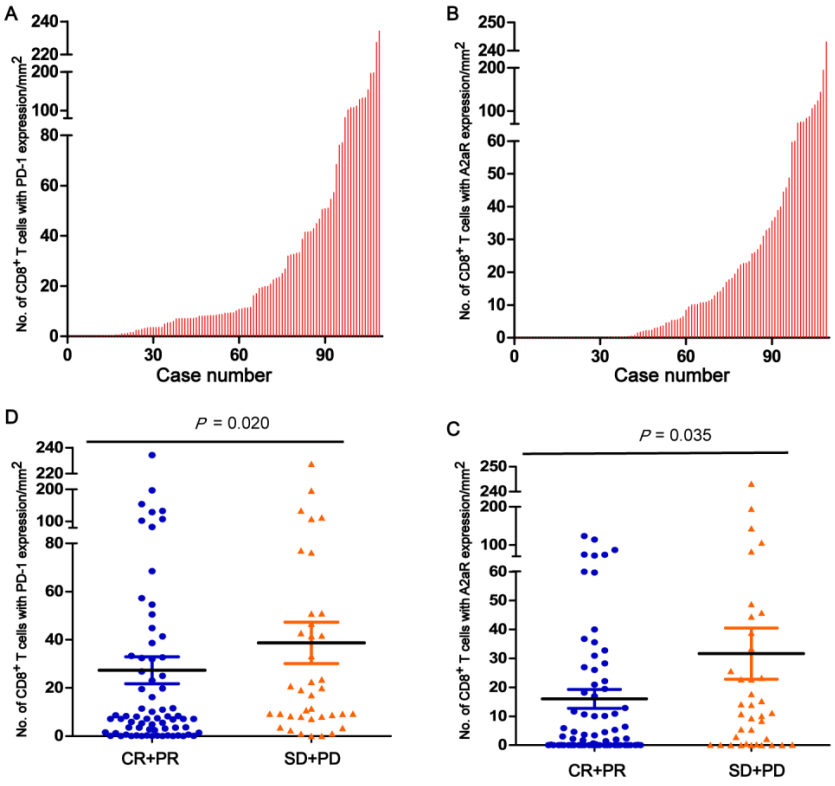

Figure S12. Correlation between PD-1 and A2aR expression on CD8$^+$ T cells and clinical responses in diffuse large B-cell lymphoma. (A-B) Numbers of CD8$^+$ T cells with PD-1 and A2aR expression per mm^2 in the overall population. The cases are ordered from lowest to highest according to cell numbers/mm^2 of PD-1 and A2aR expression. (C-D) The association between PD-1 and A2aR expression on CD8$^+$ T cells and clinical responses. CR: complete response; PR: partial response; SD: stable disease; PD: progressive disease.